ARTICLES

Test of a Chemical Timing Method for Measuring Absolute Vibrational Relaxation Rate Constants for S_1 *p*-Difluorobenzene†

Uroš S. Tasić‡ and Charles S. Parmenter*

Department of Chemistry, Indiana University, Bloomington, Indiana 47405

Received: May 28, 2004; In Final Form: November 15, 2004

A chemical timing (CT) method for measuring absolute rate constants for collisional vibrational relaxation has been tested for the 5^1 state of S_1 *p*-difluorobenzene (*p*DFB) where an alternative method exists to provide benchmark values. The CT method was originally developed to treat vibrational energy transfer (VET) in large molecules excited to high vibrational levels where the intramolecular vibrational redistribution (IVR) resulting from large vibrational state densities completely eliminates vibrational structure in the emission spectrum. Here we apply the same method to a low-lying state (5^1 with $\epsilon_{vib} = 818$ cm^{-1}) located in the low-density region of the vibrational manifold where IVR plays no role. For high vibrational levels, the chemical timing method involves addition of high O_2 pressures (kTorr) to a low-pressure *p*DFB sample, introducing vibrational structure in the fluorescence spectrum. Response of this spectrum to vibrational relaxation by Ar is then examined. For levels such as 5^1, the fully structured fluorescence spectrum allows the rate constant for single-collision VET into the surrounding vibrational field to be measured directly without the presence of O_2. The measurements of 5^1 VET have been repeated with various O_2 pressures (kTorr) for comparison with the O_2-free benchmark. In the presence of O_2, the rate constant for VET by Ar is $(4.0 \pm 0.5) \times 10^6$ Torr^{-1} s^{-1} and independent of high O_2 pressure variations. The rate constant as found by the standard O_2-free method is $(3.6 \pm 0.4) \times 10^6$ Torr^{-1} s^{-1}. This comparison suggests that the chemical timing method is capable of providing a reasonably accurate measure of the VET rate constant for high vibrational levels provided that details of the kinetics are known.

1. Introduction

We have recently described a study of collision-induced vibrational energy transfer (VET) in gas-phase S_1 *p*-difluorobenzene (*p*DFB) with high vibrational energy ($\epsilon_{vib} = 3700$ cm^{-1}) where the large state density ($\rho_{vib} > 10^4$ states per cm^{-1}) creates a vibrational quasi-continuum.[1] That study is part of a series aimed at measuring the absolute VET rate constants for increasingly higher vibrational energies.[2,3] The constants concern VET from an initially pumped level (or region) to the surrounding S_1 vibrational field.

Our motivation for determining such constants is provided by the opportunity to learn about the magnitude of VET rate constants for the high vibrational energies associated with molecules thermally activated for reaction. Much is known about the collisional processes of activation/deactivation such as the average state-to-field energy change per collision or the energy transfer distribution functions.[4−9] These quantities are usually derived with modeling of the experimental results that requires an absolute state-to-field VET rate constant to normalize the modeling to a per collision basis. However, no such rate constant has ever been measured. In the absence of experimental values, Lennard-Jones rate constants are usually assumed.[10−13]

It is anticipated that the pattern of our experimental VET rate constants obtained as higher and higher initial levels are pumped would be instructive on this issue. As part of this effort, state-to-field VET rate constants for initial S_1 vibrational energies below $\epsilon_{vib} = 3700$ cm^{-1} were obtained by monitoring vibrational band intensities in S_1-S_0 fluorescence when a gas such as Ar is added to the fluorescence cell containing *p*DFB.[2,3] A problem arises, however, for S_1 levels with $\epsilon_{vib} = 3700$ cm^{-1} or higher. The vibrational band structure needed for VET measurements is missing in the fluorescence because of extensive intramolecular vibrational redistribution (IVR).

We have developed a new method to make rate constant measurements possible for these high levels.[1] The technique uses high added O_2 pressures (kTorr) that introduce vibrational structure into the structureless spectrum as the fluorescence is increasingly quenched by S_1 state destruction. The approach may be recognized as a derivative of the chemical timing (CT) approach used to study of IVR in aromatic molecules.[14−16] In its adaptation to VET, the CT-VET method, as it might be termed, enables us to investigate high-energy vibrational regions that have never before been accessible.

Since the CT-VET method creates a severe system perturbation associated with high O_2 pressures and fluorescence quenching, an obvious question arises. How reliable are such absolute VET rate constants? To answer this question, we have gone back to a low-lying vibrational level that has already been the

† Part of the special issue "George W. Flynn Festschrift".

* Author to whom correspondence should be addressed. Fax: (812) 855-8300. E-mail: parment@indiana.edu.

‡ Present address: Department of Chemistry, Texas Tech University, Lubbock, TX 79409

10.1021/jp040396r CCC: $30.25 © 2005 American Chemical Society
Published on Web 02/12/2005

subject of an extensive investigation by the standard VET technique[2,3,17,18] and that therefore provides a benchmark for our CT method. The particular state is 5^1 *p*DFB with $\epsilon_{vib} = 818\ cm^{-1}$ where IVR is absent and the vibrational state density is sparse so that the states do not overlap. The rate constant for state-to-field VET by Ar collisions is well-known for this state. Now we want to measure the same quantity with the CT-VET method.

Both the chemical timing and the standard approach to the VET rate constant measurements are based on the straightforward use of an optical pump and a fluorescence probe.[17] An initial S_1 vibrational state is selected by tuned laser pumping, and a vibrational band intensity in the ensuing $S_1 \rightarrow S_0$ fluorescence spectrum is monitored as the molecules are brought increasingly into interactions with the added VET gas, Ar in this case. In the standard approach, the collision-free fluorescence lifetime[19] provides an internal clock for establishing absolute rate constants under single-collision conditions. In the chemical timing experiments, this clock is provided by O_2 collisions via electronic quenching. The former clock is useful for timing events on the few nanosecond time scale, while the latter is widely tunable, up to the picosecond time scale.

There is no new dynamic information to be learned from the present study, but it provides an opportunity to combine all our knowledge about the 5^1 state VET and apply it into the much more complicated environment of CT-VET experiments. By analogy to our CT-VET study[1] at $\epsilon_{vib} = 3700\ cm^{-1}$, we perform experiments at a range of high (kTorr) O_2 pressures. The electronic quenching kinetics with O_2 are already known and will be used with various details about the state-to-state VET propensities in our analysis.

As we will show, the CT-VET method, operating with collision conditions very different than those of a standard VET study, is not a simple extension of the standard method but requires substantial modification of the kinetic scheme. We shall also see that a low-lying state such as 5^1 is fundamentally different from the high-lying level that was the subject of our earlier report.[1] Some alterations in the analysis of the CT-VET method itself are necessary to bridge these two regions of the vibrational manifold. Most importantly, because the number of states surrounding 5^1 is relatively small, we have to be concerned about feedback into the 5^1 state by multiple collisions under the high-pressure conditions of the CT-VET experiments.

2. Experimental Procedure

The experimental setup is essentially the same as that described earlier.[3] Briefly, an Nd:YAG laser-pumped dye laser with frequency doubling is used to prepare *p*DFB into the 5^1 vibrational state by the 5_0^1 transition. The sample is contained in a static cell at 300 K. The standard VET experiment involves a sample of 60−80 mTorr *p*DFB to which 1−6 Torr Ar is incrementally added. In the CT-VET experiments, we incrementally add Ar to a mixture of 0.3−0.5 Torr of *p*DFB with 50−7000 Torr of O_2 at constant partial pressures. Fluorescence is collected normal to the incident laser beam and imaged into a monochromator operated with roughly 45 cm^{-1} resolution. The monochromator is set to select one of the two fluorescence transitions $5_0^1 6_1^0$ or $5_0^1 6_2^0$.[20] Figure 1 shows a segment of the fluorescence spectrum containing these bands. The band intensities during Ar additions provide two independent values of the fluorescence signal. The signal is averaged for each Ar increment. A single experiment at a given O_2 pressure consists of acquiring the signals at 7 to 11 added Ar pressures.

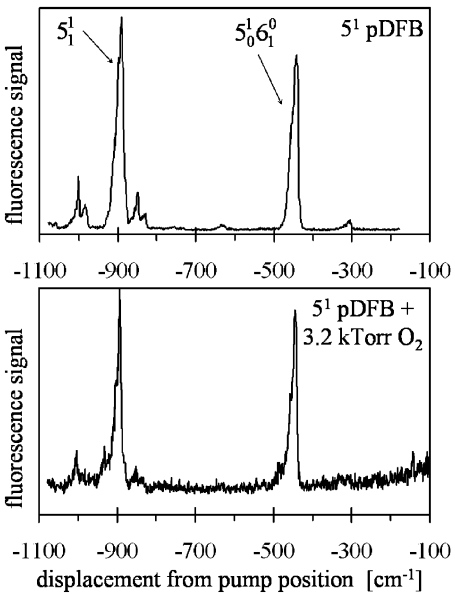

Figure 1. A segment of the collision-free single vibronic level fluorescence spectrum of 5^1 *p*DFB indicating the positions of two band maxima that are monitored in the VET experiments. Upper plot is for neat *p*DFB, and the lower plot is for *p*DFB in the presence of 3.2 kTorr of O_2. The features with O_2 are much weaker than under collision-free conditions, but the emission profile is essentially the same. The displacement is from the pump position at 37 658 cm^{-1}.

3. Kinetic Mechanism

The sample in the CT-VET experiments is a three-component mixture with the *p*DFB target gas at relatively low pressure and with O_2 and Ar at relatively high pressures. The number of possible destination states for VET with Ar is rather small, with one of the channels being particularly efficient.[17,18] This special channel involves a transition to the nearby upper state $5^1 30^1$. That state has a pronounced propensity[18] to reform the 5^1 state upon a subsequent collision with a loss of a quantum of $\nu'_{30} = 122\ cm^{-1}$. The situation is further complicated by the fact that O_2 provides 5^1 *p*DFB with at least three destruction channels, some of which are also reversible. Oxygen has VET pathways similar to those with Ar plus two channels for electronic quenching.[21]

Table 1 summarizes the most relevant processes characterizing our system in the CT-VET experiment, where index "i" refers to the 5^1 state, "j" refers to $5^1 30^1$ state, and "f" refers to the field of all other neighboring S_1 vibrational states. Figure 2 contains a schematic of the mechanism. The elementary kinetic processes listed in Table 1 encompass three types of S_1 *p*DFB species, the initially pumped 5^1 state labeled B, the $5^1 30^1$ state labeled B* and lying 122 cm^{-1} above 5^1, and the surrounding field of S_1 states labeled B**. The first three processes in Table 1 combine collision-free radiative and nonradiative electronic decay. Processes 4−6 represent electronic quenching of each *p*DFB species by O_2. The electronic quenching rate constants do not show a significant dependence on vibrational state so that we assign the same $k_q^{B^*}$ value to the 5^1 and the $5^1 30^1$ states. Since B** represents a large field of states rather than a single state, it has a different effective electronic quenching constant $k_q^{B^*}$ in accordance with our earlier finding that there are two distinct mechanisms of electronic quenching.[21] The remaining processes in Table 1 concern VET. For each VET process with Ar, there is a corresponding process with O_2. The 5^1 state has two types of VET channels. It can reversibly form the $5^1 30^1$ state B* or irreversibly disappear into the field of neighboring vibrational states B**.

TABLE 1: Process that Constitutes the CT-VET Kinetic Model[a]

	processes	rate constant	description
1	$B \rightarrow S_0 + h\nu_f$	k_f	fluorescence[b]
2	$B^* \rightarrow S_0 + h\nu_f$	k_f	fluorescence[b]
3	$B^{**} \rightarrow S_0 + h\nu_f$	k_f	fluorescence[b]
4	$B + O_2 \rightarrow ...$	$k_q^{B^*}$	electronic quenching[c]
5	$B^* + O_2 \rightarrow ...$	$k_q^{B^*}$	electronic quenching[c]
6	$B^{**} + O_2 \rightarrow ...$	$k_q^{B^{**}}$	electronic quenching[c]
7	$B + O_2 \rightarrow B^{**} + O_2$	$k_{if}^{O_2}$	VET
8	$B + Ar \rightarrow B^{**} + Ar$	k_{if}^{Ar}	VET
9	$B + O_2 \rightarrow B^* + O_2$	$k_{ij}^{O_2}$	VET
10	$B + Ar \rightarrow B^* + Ar$	k_{ij}^{Ar}	VET
11	$B^* + O_2 \rightarrow B^{**} + O_2$	$k_{jf}^{O_2}$	VET
12	$B^* + Ar \rightarrow B^{**} + Ar$	k_{jf}^{Ar}	VET
13	$B^* + O_2 \rightarrow B + O_2$	$k_{ji}^{O_2}$	VET
14	$B^* + Ar \rightarrow B + Ar$	k_{ji}^{Ar}	VET

[a] B represents the pumped 5^1 S_1 *p*DFB state; B* represents the 5^130^1 state; B** represents the field of S_1 levels surrounding B and B*. [b] $k_f = 1.0 \times 10^8$ s^{-1}, ref 19. [c] $k_q^{B^*} = 8.0 \times 10^6$ $Torr^{-1}$ s^{-1}, ref 21. [d] $k_q^{B^{**}} = 0.99 \times 10^6$ $Torr^{-1}$ s^{-1}, ref 21.

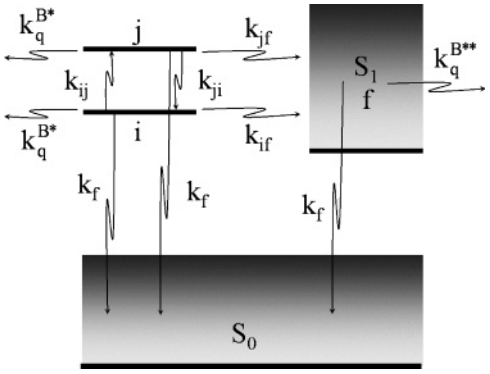

Figure 2. Kinetic scheme for CT-VET experiments. The state i refers to 5^1, j refers to 5^130^1, and f refers to the field of neighboring vibrational states.

Electronic quenching with increasing O_2 pressure is responsible for a general drop in total fluorescence intensity and also for redistribution of fluorescence intensity within the emission spectrum due to VET. The monitored fluorescence intensity I_{Ar} of vibrational bands represents the population of the fluorescing 5^1 state. Although all 5^1 destruction processes contribute to a decrease in signal at larger O_2 and Ar pressures, their net effect is somewhat diminished by the reverse $5^1 \leftarrow 5^130^1$ VET channel represented by processes 13 and 14.

Several relationships among the elementary steps simplify the kinetic analysis. The state-to-field VET rate constants for the 5^1 and 5^130^1 states with Ar and O_2 partners do not explicitly show up in Table 1, but they are the ultimate rate constants we seek from this study. The constants are designated k_i^M for the 5^1 state and k_j^M for 5^130^1, with M = Ar or O_2. These constants are related to other VET rate constants listed in Table 1 by

$$k_i^{Ar} = k_{ij}^{Ar} + k_{if}^{Ar} \qquad k_i^{O_2} = k_{ij}^{O_2} + k_{if}^{O_2}$$

$$k_j^{Ar} = k_{ji}^{Ar} + k_{jf}^{Ar} \qquad k_j^{O_2} = k_{ji}^{O_2} + k_{jf}^{O_2} \tag{1}$$

The special state-to-field VET channel $5^1 \leftrightarrow 5^130^1$ is associated with the forward and reverse rate constants related via microscopic reversibility[18] as shown in eq 2.

$$\beta = \frac{k_{ji}^{Ar}}{k_{ij}^{Ar}} = \frac{k_{ji}^{O_2}}{k_{ij}^{O_2}} = \exp\left(\frac{E_j - E_i}{k_B T}\right) = 1.80 \tag{2}$$

The Boltzmann factor value β comes from the 122 cm^{-1} energy difference between the 5^1 and 5^130^1 states at 22 °C.

The special state-to-state VET channel and state-to-field VET are also related. The former is associated with a specific value[18,22] that is independent of the initial state for low-lying states. In particular, analysis of these state-to-state VET rate constants reveals a generic value of $k_{ji}^{Ar} = 2.9 \times 10^6$ $Torr^{-1}$ s^{-1} for the loss of a quantum of v'_{30} in collisions with Ar.[18] The associated rate constant for the gain of a quantum of v'_{30} is $k_{ij}^{Ar} = 1.6 \times 10^6$ $Torr^{-1}$ s^{-1} via microscopic reversibility.

Finally, we note that state-to-field VET rate constants by Ar and by O_2 are related approximately by a parameter γ as given by

$$\gamma = k_i^{O_2}/k_i^{Ar} = k_j^{O_2}/k_j^{Ar} = 0.59 \tag{3}$$

The parameter γ represents the VET efficiency of O_2 relative to the Ar partner. It is assumed to be the same for the 5^1 and 5^130^1 states. The value of γ is known from an earlier explicit experimental investigation of VET by O_2.[23]

The above relationships allow us to manage the kinetic scheme in Table 1 and obtain an expression for the fluorescence band intensity I_{Ar}. The expression is

$$\frac{\Omega}{I_{Ar}} = k_f + k_i^{Ar}P + k_q^{B^*}[O_2] - \frac{(k_{ji}^{Ar}P)^2/\beta}{k_f + (k_i^{Ar} + k_{ji}^{Ar})P + k_q^{B^*}[O_2]} \tag{4}$$

where Ω is an instrumental constant and where P refers to the effective pressure of VET-inducing gas. P is

$$P = [Ar] + \gamma[O_2] \tag{5}$$

Equation 4 is clearly nonlinear in Ar. That nonlinearity is a consequence of the reversible state-to-state VET channel. Values of all parameters and rate constants in eq 4 are known except for the rate constant k_i^{Ar} that we seek. The test of CT-VET experiments described by eq 4 then involves measuring k_i^{Ar} at fixed O_2 pressures and comparing it with the known value determined by standard O_2-free VET experiment. If the kinetic model of CT-VET is correct, then the same values of k_i^{Ar} should result *regardless of the O_2 pressure*, and it should match the value determined in the absence of O_2 by the standard VET method.

If there was no special state such as 5^130^1 with its pronounced reversible VET channel, then one could ignore reformation of the 5^1 state by letting the rate constant for the $5^1 \leftarrow 5^130^1$ channel be zero. For this situation, the expression in eq 4 simplifies into that given by

$$\frac{\Omega}{I_{Ar}} = k_f + k_i^{Ar}P + k_q^{B^*}[O_2] = k_f + (\gamma + k_q^{B^*})[O_2] + k_i^{Ar}[Ar] \tag{6}$$

Now the inverse signal has a linear Stern−Volmer-like dependence on the Ar pressure.

4. Results

Electronic quenching of 5^1 fluorescence by high O_2 pressure does not qualitatively alter the fluorescence spectrum. In Figure

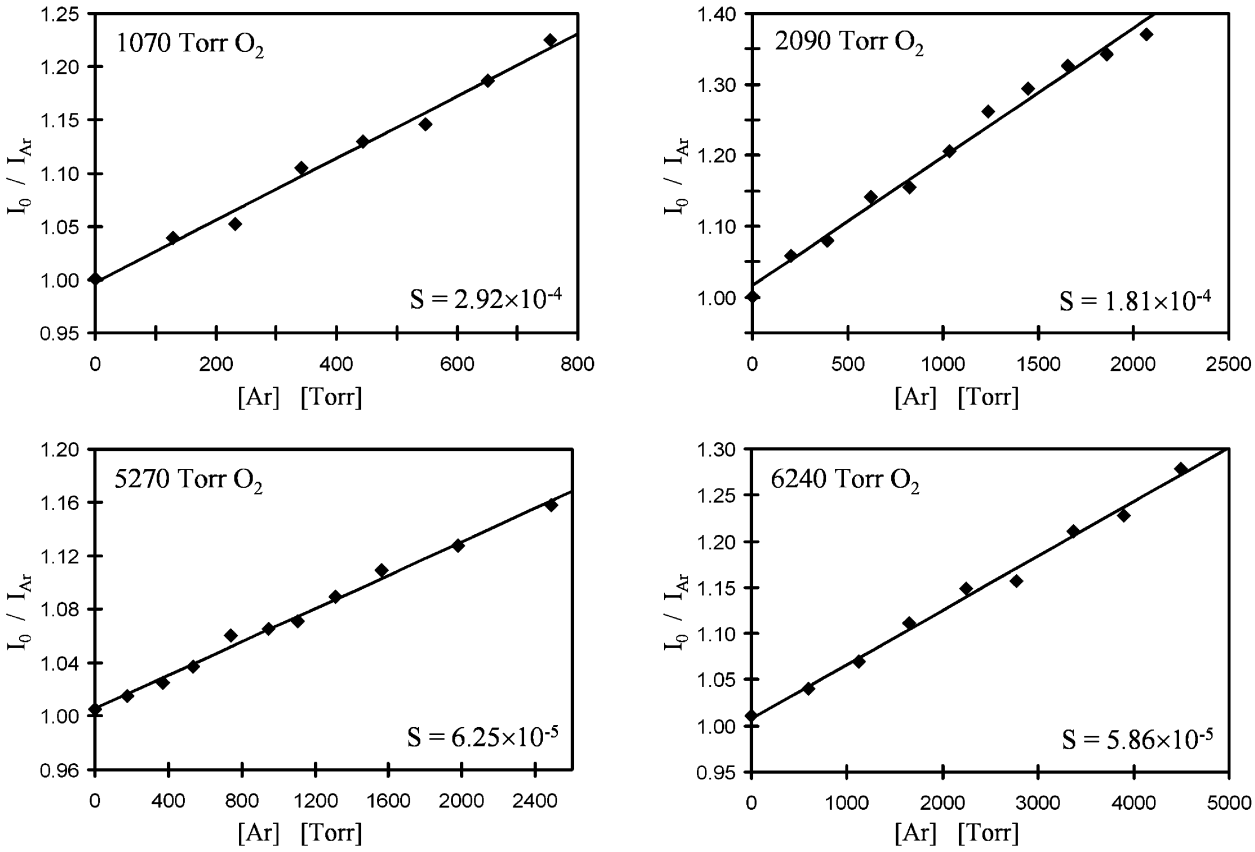

Figure 3. Stern−Volmer plots for 5^1 *p*DFB + Ar CT-VET experiments using various O_2 pressures.

1, we display a spectrum obtained under O_2-free conditions and one under a high O_2 pressure. The structured features observed in the spectrum at high O_2 pressure correspond to the same vibronic transitions seen in the O_2-free spectrum. In contrast, the 5^1 emission spectrum completely transforms due to VET under an equally high Ar pressure. This observation is consistent with the electronic quenching ability of O_2 and the absence of quenching by Ar.

Figure 3 shows representative results of monitoring the bands in Figure 2 under constant O_2 pressure and varying Ar pressures. Each Stern−Volmer plot shows the ratio of fluorescence signal intensities I_0/I_{Ar} without and with added Ar versus the Ar pressure. The O_2 pressure is fixed during each experiment and is indicated together with the least-squares linear fit slope *S*. Such Stern−Volmer plots are available for 12 different CT-VET experiments at various O_2 pressures. All experiments regardless of O_2 pressure are performed with enough Ar to produce a significant drop in fluorescence intensity. However, Ar pressures are limited to avoid making the kinetic model more complicated by multiple VET collisions with Ar. This balance between pressure requirements typically means a drop of up to about 20% in fluorescence intensity at the highest Ar pressure, which is approximately the O_2 pressure.

Although the inverse signal Ar is expected to be nonlinear with Ar pressure, this nonlinearity is in fact quite small (under 3%) and cannot be discerned from random error because of the limited Ar pressure range. An analysis shows, however, that neglecting the $5^1 \leftarrow 5^1 3^0 1^1$ repopulation channel would lead to an approximately 12% underestimate of the k_i^{Ar} value, independent of oxygen pressure for our higher O_2 pressure. For this reason, although the Stern−Volmer data are fitted with a straight line, the resulting slope *S* is analyzed via eq 4 so as to determine the VET rate constant with Ar at each O_2 pressure.

TABLE 2: 5^1 *p*DFB + Ar State-to-Field VET Rate Constants as a Function of [O_2] as Observed in CT-VET Experiments

[O_2] (Torr)	S^a (10^{-4} Torr^{-1})	k_i^{Ar} (10^6 Torr^{-1} s^{-1})^b
53	40.2	2.96
268	12.6	4.04
1070	2.92	3.64
1070	3.31	4.13
1830	2.05	4.34
1940	2.09	4.84
2090	1.81	4.46
2120	1.39	3.44
3160	1.18	4.31
5270	0.625	3.78
6240	0.586	4.26
7290	0.480	4.04

[a] Observed slope of plots such as those in Figure 3. [b] Average of the column = 4.0×10^6 Torr^{-1} s^{-1} with a standard deviation of0.52×10^6 Torr^{-1} s^{-1} (13%).

The extracted state-to-field rate constants k_i^{Ar} are summarized in Table 2 together with the Stern−Volmer slopes for the various O_2 pressures at which the experiments are performed. All parameters in eq 4 are already known ($k_f = 1.0 \times 10^8$ s^{-1}, $k_q^{B^*} = 8.0 \times 10^6$ Torr^{-1} s^{-1}, $\beta = 1.80$, $\gamma = 0.59$, and $k_{ji}^{Ar} = 2.9 \times 10^6$ Torr^{-1} s^{-1}) so that the desired 5^1 + Ar state-to-field VET rate constant k_i^{Ar} is the only unknown. That constant is found by performing the best fit to eq 4 that reproduces the experimentally measured slope. The average of the CT-VET rate constants in Table 2 is $k_i^{Ar} = (4.0 \pm 0.52) \times 10^6$ Torr^{-1} s^{-1} where the uncertainty is the standard deviation from the mean of the set. Since the rate constants show no systematic dependence on O_2, the 12 values in Table 2 can be considered as independent determinations with a precision given by the standard deviation.

TABLE 3: VET Rate Constants from Classic and Chemical Timing VET Measurements

	k_i^{Ar} (10^6 Torr^{-1} s^{-1})
classic VET[a]	4.0
classic VET[b]	3.3
classic VET[c,d]	3.5
CT-VET	4.0

[a] From Catlett, D. L., Jr., Ph.D. Thesis, Indiana University, 1985. [b] From ref 3. [c] From ref 23. [d] Average of the three classic VET values = 3.6×10^6 Torr^{-1} s^{-1} with a standard deviation of 0.29×10^6 Torr^{-1} s^{-1} (8.2%).

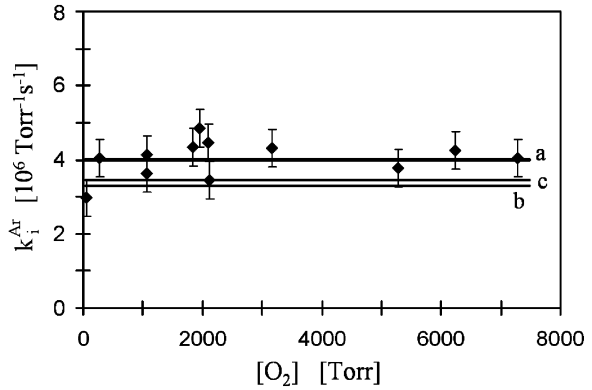

Figure 4. Plot of 5^1 *p*DFB + Ar state-to-field VET rate constants k_i^{Ar} from CT-VET experiments (points) (Table 2) and from the conventional O_2-free experiments (lines a, b, and c) (Table 3). Each error bar is the standard deviation of the set of CT-VET determinations as given in Table 2.

To provide a benchmark value of k_i^{Ar} without added O_2, three independent measurements with $[O_2] = 0$ were performed by the above techniques. The average of these O_2-free VET measurements is $k_i^{Ar} = 3.45 \times 10^6$ Torr^{-1} s^{-1} with a standard deviation of 0.21×10^6 Torr^{-1} s^{-1}.

5. Discussion

The purpose of these experiments is to test the validity of the CT-VET experiments. Since they measure absolute state-to-field VET rate constants of S_1 *p*DFB in the midst of high (kTorr) O_2 pressures, there is opportunity to obtain a rate constant that differs from the true value of an O_2-free system. For example, the rate constant may be intrinsically perturbed by the *p*DFB interactions with O_2. Alternatively, the derived rate constant may be in error as a result of shortcomings in the kinetic mechanisms or of incorrect values of parameters used in the kinetic analysis.

The state-to-field rate constants from the S_1 *p*DFB state 5^1 obtained under high O_2 pressures are listed in Table 2 for oxygen pressures in roughly the range 60−7000 Torr. Their average $k_i^{Ar} = (4.0 \pm 0.5) \times 10^6$ Torr^{-1} s^{-1} can be compared with k_i^{Ar} values found by the standard O_2-free VET experiments. The measurement in this work is joined by two made by others. The values of these three independent measurements are listed in Table 3. The resulting rate constant $k_i^{Ar} = (3.6 \pm 0.3) \times 10^6$ Torr^{-1} s^{-1} agrees with those from the CT-VET experiments.

This agreement is perhaps best illustrated in Figure 4 where the 12 values of 5^1 VET rate constants from the CT-VET experiments are plotted against the O_2 pressure at which the experiments were performed. The plot also contains the three independent standard measurements that serve as the reference values (the lines a, b, and c). Although the CT-VET data have some scatter, they show no dependence on the O_2 pressure, and their average matches the reference values within the random error. The three independent reference values (Table 3) have an 8% standard deviation from their mean. The larger standard deviation (13%) of the CT-VET method is partially the result of the much smaller fluorescence signals under high O_2 pressures and of more complicated collision conditions in the cell. The other sources of random error are common with those of classic method.

One might ask whether the k_i^{Ar} rate constant should depend on the O_2 pressure under widely different collision conditions. For example, under O_2-free conditions, the VET collision with Ar occurs at 1−10 ns after 5^1 preparation, while under several kTorr O_2 pressure the Ar collision occurs at 10−100 ps after 5^1 preparation. Regardless of when the *p*DFB encounter with Ar occurs, it could be consequential on the k_i^{Ar} value only if the prepared 5^1 state has evolved to other states. Since our probe is a vibronic transition of the fluorescence spectrum, it is specific only to *p*DFB in the 5^1 state. Thus the experiment is blind to Ar collisions with all other states so that it is irrelevant whether 5^1 *p*DFB encounters Ar at 10 ns or at 10 ps after its preparation. The k_i^{Ar} value is characteristic of the 5^1 *p*DFB collisional interaction with Ar, independent of pressure conditions.

As seen from Table 3 and Figure 4, the major conclusion from this series of CT-VET experiments is that, given the appropriate kinetic model and parameters, the CT-VET technique can be used to determine a valid state-to-field VET rate constant. Its precision is somewhat sacrificed, and the accuracy depends on the reliability of other kinetic parameters that must be measured independently such as rate constants for the electronic quenching and the O_2 VET.

There are three special cases of the kinetic scheme in Figure 2 worth considering; (i) one can let $k_{ji}^{Ar} = 0$ and thereby ignore repopulation of the state 5^1, (ii) one can treat O_2 as an ideal electronic quencher by letting $k_i^{O_2} = 0$, or (iii) one can try to apply both approximations. It turns out that neglecting the $5^1 \leftarrow 5^1 3 0^1$ feedback channel reduces the k_i^{Ar} value from 4.0×10^6 Torr^{-1} s^{-1} by about 12% to 3.5×10^6 Torr^{-1} s^{-1}, which still agrees well with the mean of the O_2-free reference values (3.6×10^6). Clearly, repopulation of 5^1 does not have a major effect on accuracy. However, ignoring the ability of O_2 to induce VET has a larger effect. It reduces the k_i^{Ar} value to 3.0×10^6 Torr^{-1} s^{-1}. Applying both approximations reduces the k_i^{Ar} value to 2.8×10^6 Torr^{-1} s^{-1}. Note that we use 8.0×10^6 Torr^{-1} s^{-1} as the electronic quenching rate constant. A second value $k_q^{B^*} = 7.2 \times 10^6$ Torr^{-1} s^{-1} is available from other independent measurements.[21] With this lower value, all the above k_i^{Ar} values from CT-VET experiments drop by about 7%. Use of the $k_{ji}^{Ar} = 0$ approximation with the lower $k_q^{B^*}$ value still yields a good k_i^{Ar} value, but the $k_i^{O_2} = 0$ approximation yields a significant underestimate. Additional refinements to the kinetic model in Figure 2 would not be productive in view of existing random error in CT-VET experiments and uncertainty in values of various contributing rate constants.

The results of this exploration of 5^1 VET in the presence of high O_2 pressures also provide evidence that the kinetic model is appropriate in its principal features. By the combination of various ideas and known parameters into a model for a system far more complex than that of the classic VET experiments, the agreement of rate constants demonstrates in turn that concepts incorporated in the CT-VET model used for high vibrational levels are valid.

The O_2 quenching kinetics is of particular concern in the modeling of CT-VET. Our recent study of quenching kinetics[21]

revealed a complicated mechanism that contains two quenching rate constants differing from each other by an order of magnitude. A valid CT-VET rate constant requires correct use of these kinetics, and the success of this test of CT-VET versus the classic VET experiment indicates that the O_2 quenching kinetics are understood.

A more specific note on the oxygen quenching kinetics is warranted since the quenching plays such a central role in the CT-VET method. According to the model developed recently,[21] the two rate constants are associated with different routes for electronic quenching. One route proceeds via an excited *p*DFB·O_2 intermediate complex that, among other things, can dissociate to regenerate the S_1 state upon a second encounter with O_2. The S_1 vibrational state destinations of this channel are unknown, but we assume that only a small fraction of these events can repopulate the original 5^1 state. With this assumption, the $k_q^{B^*}$ value used in our analysis above is the sum of rate constants for both quenching channels. In the opposite case, a highly unlikely scenario, the $k_q^{B^{**}}$ value would be used instead. This value corresponds to the direct $S_1 \rightarrow T_1$ quenching channel and is much smaller. This reduction in the electronic quenching rate constant would lower the k_i^{Ar} value extracted from CT-VET experiments far below the reference values.

The purpose of these experiments is to test the CT-VET method so it can be applied to high-lying vibrational levels. There is however a significant difference between the 5^1 and high-lying states, and one may wonder how appropriate this test is for levels with $\epsilon_{vib} > 3300$ cm^{-1}. The low-lying states such as 5^1 are characterized by simple structured emission spectra, strong transitions, strong selection rules, and a limited number of neighboring vibrational states. This implies a need for an involved kinetic scheme with understanding of the relationship among the few VET destination states, as presented in Figure 1. As one climbs to high-lying vibrational levels with $\epsilon_{vib} > 3300$ cm^{-1} where we now must use the CT-VET technique, the net effective kinetic scheme actually becomes simplified. The reversible VET channel loses its significance due to the loss of the $\Delta v_{30} = 1$ VET channel dominance because of the dilution of the zero-order character of vibrational states.[24] As one climbs to even higher levels, the quantum state sensitivity is expected to diminish even further so that any repopulation of the initially prepared state must be insignificant. Extensive IVR in high-lying states is another key difference between the two vibrational domains. Inclusion of IVR in the kinetic scheme for the high levels is easily accommodated.

6. Summary

A series of state-to-field VET studies provides VET rate constants for S_1 *p*DFB in collision with rare gases. The rate constants are measured for initial levels of higher and higher energy to gain information about the virtue of using Lennard-Jones rate constants in the modeling of the activation/deactivation steps in thermal unimolecular reactions. The observed S_1 *p*DFB rate constants increase with increasing energy for the lower initial vibrational levels. The question is whether the increasing rate constants ultimately level off at higher energies and, if they do, what is their magnitude at that point.

The VET studies for lower levels are based on straightforward monitoring of vibrational band intensities in S_1-S_0 fluorescence. The studies have now reached higher levels where extensive level mixing and level overlap occurs due to the large vibrational state densities. IVR in these regions eliminates all vibrational structure in the fluorescence so that a new method is required to study the VET. The method is based on chemical timing of fluorescence with large pressures (kTorr) of O_2 that introduce structure into the fluorescence along with quenching. The present study is in part a test of whether accurate VET rate constants can be obtained in the midst of the perturbations associated with the severe collisional environment of high O_2 pressures. The test is provided by measuring the rate constant in the presence of added O_2 for a low level whose rate constant is already well-known from low-pressure studies using the conventional method. The chosen level is the 5^1 fundamental at $\epsilon_{vib} = 818$ cm^{-1}. It lies in a relatively sparse state density region where IVR is absent and levels are well-described with a simple and (nearly) unmixed harmonic basis.

The VET rate constants for the 5^1 level obtained in the presence of various fixed O_2 pressures between about 60 and 7000 Torr show no dependence on the O_2 pressure. The average value of these determinations is 4.0×10^6 Torr^{-1} s^{-1} (Table 2). That value can be compared with the average 3.6×10^6 Torr^{-1} s^{-1} of three independent O_2-free studies (Table 3). The two averages lie within the standard deviations of their means. These results suggest that valid rate constants are produced by the CT-VET method.

These studies also provide confidence that the rather complicated kinetics of O_2 fluorescence quenching discovered[21] for S_1 *p*DFB are correctly interpreted. The quenching involves two channels for S_1 destruction with quenching rate constants differing by about an order of magnitude. Further, one of these channels is reversible under an ensuing O_2 collision. Without application of the correct O_2 quenching kinetics to the 5^1 CT-VET modeling, agreement between the two types of experiments would not have been obtained.

The studies also indicate that the state-to-state VET of low levels is correctly characterized. The high-pressure environment of the CT-VET experiment for 5^1 involves modeling that includes a reversible state-to-state channel concerning a quantum change in the lowest frequency S_1 *p*DFB mode $\nu'_{30} = 122$ cm^{-1}. Past state-to-state studies[17,18] characterized this channel and determined the rate constants for numerous low S_1 *p*DFB levels, including 5^1 S_1 *p*DFB. As with the case of the O_2 quenching kinetics, agreement between CT-VET and conventional VET experiments is dependent on correct analysis of this special channel's role in S_1 *p*DFB VET.

Acknowledgment. We are grateful to the National Science Foundation for financial support of this work. It is a special pleasure for C.S.P. to join others in this Festschrift honoring George Flynn. Professor Flynn's vibrational explorations and friendship have been inspiring for many years.

References and Notes

(1) Tasic, U. S.; Parmenter, C. S. *J. Phys. Chem. B* **2004**, *108*, 10325.
(2) Catlet, D. L., Jr.; Parmenter, C. S.; Pursell, C. J. *J. Phys. Chem.* **1995**, *99*, 7371.
(3) Stone, T. A.; Parmenter, C. S. *J. Phys. Chem. A* **2002**, *106*, 938.
(4) Seiser, N.; Kavita, K.; Flynn, G. W. *J. Phys. Chem. A* **2003**, *107*, 8191.
(5) Weston, R. E.; Flynn, G. W. *Annu. Rev. Phys. Chem.* **1992**, *43*, 559.
(6) Flynn, G. W.; Parmenter, C. S.; Wodtke, A. M. *J. Phys. Chem.* **1996**, *100*, 12817.
(7) Park, J.; Lawrence, S.; Lemoff, A. S.; Werner, K.; Mullin, A. S. *J. Chem. Phys.* **2002**, *117*, 5221.
(8) Barker, J. R.; Toselli, B. M. *Int. Rev. Phys. Chem.* **1993**, *12*, 305.
(9) Kappel, C.; Luther, K.; Troe, J. *Phys. Chem. Chem. Phys.* **2003**, *4*, 4392.
(10) Goos, E.; Hippler, H.; Kachiani, C.; Svedung, H. *Phys. Chem. Chem. Phys.* **2002**, *4*, 4372
(11) Barker, J. R.; Ortiz, N. F. *Int. J. Chem. Kinet.* **2001**, *33*, 246.
(12) Bernshtein, V.; Oref, I. *J. Chem. Phys.* **1998**, *108*, 3543.

(13) Elioff, M. S.; Wall, M. C.; Mullin, A. S. *J. Chem. Phys.* **1999**, *110*, 5578.
(14) Coveleskie, R. A.; Dolson, D. A.; Parmenter, C. S. *J. Phys. Chem.* **1985**, *89*, 645.
(15) Coveleskie, R. A.; Dolson, D. A.; Moss, D. B.; Munchak, S. C.; Parmenter, C. S. *Chem. Phys.* **1985**, *96*, 191.
(16) Holtzclaw, K. W.; Parmenter, C. S. *J. Chem. Phys.* **1986**, *84*, 1099.
(17) Catlett, D. L., Jr.; Parmenter, C. S. *J. Phys. Chem.* **1991**, *95*, 2864.
(18) Catlett, D. L., Jr.; Parmenter, C. S.; Pursell, C. J. *J. Phys. Chem.* **1994**, *98*, 3263.
(19) Guttman, C.; Rice, S. A. *J. Chem. Phys.* **1974**, *61*, 661.
(20) Coveleskie, R. A.; Parmenter, C. S. *J. Mol. Spectrosc.* **1981**, *86*, 86.
(21) Tasić, U. S.; Davidson, E. R.; Parmenter, C. S. *J. Phys. Chem. A* **2003**, *107*, 3552.
(22) Krajnovich, D.; Catlett, D. L., Jr.; Parmenter, C. S. *Chem. Rev.* **1987**, *87*, 237.
(23) Tasić, U. S. Ph.D. Thesis, Indiana University, 2004.
(24) Dolson, D. A.; Holtzclaw, K. W.; Moss, D. B.; Parmenter, C. S. *J. Chem. Phys.* **1986**, *84*, 1119.